

A Time-Frequency Classifier for Human Gait Recognition

Bijan G. Mobasseri^a and Moeness G. Amin^b

^aElectrical and Computer Engineering Department, Villanova University, Villanova, PA;

^bCenter for Advanced Communications, Villanova University, Villanova, PA

ABSTRACT

Radar has established itself as an effective all-weather, day or night sensor. Radar signals can penetrate walls and provide information on moving targets. Recently, radar has been used as an effective biometric sensor for classification of gait. The return from a coherent radar system contains a frequency offset in the carrier frequency, known as the Doppler Effect. The movements of arms and legs give rise to micro Doppler which can be clearly detailed in the time-frequency domain using traditional or modern time-frequency signal representation. In this paper we propose a gait classifier based on subspace learning using principal components analysis(PCA). The training set consists of feature vectors defined as either time or frequency snapshots taken from the spectrogram of radar backscatter. We show that gait signature is captured effectively in feature vectors. Feature vectors are then used in training a minimum distance classifier based on Mahalanobis distance metric. Results show that gait classification with high accuracy and short observation window is achievable using the proposed classifier.

Keywords: Gait classification, Doppler, Time-Frequency

1. INTRODUCTION

Recent focus on technologies serving homeland security and rescue operations have prompted interest in the evaluation of the human body radar signature. This is motivated by the fact that vision-based approaches for detection, tracking and classifications of human motions¹ are not typically possible in urban sensing applications due to presence of walls and other obstructions. Even in open space using visual sensors the perception of motion is often difficult due to variations in lighting, deformations of clothing, and the size of person in the scene.²

Radar has established itself as an effective all-weather, day or night sensor. Radar signals can penetrate walls and provide velocity of moving targets whether the motion is linear, vibrational, or rotational. The return from a coherent radar system contains a frequency offset in the carrier frequency, known as the Doppler Effect. This shift captures the velocity of the target. Mechanical vibrations or rotations of a target induce additional frequency modulations on radar returns, which generate sidebands about the Doppler frequency, referred to as micro Doppler effect. Targets or structures on targets may have rotations, vibrations, or translations motions or combinations of these motions in three- or two-dimensional space.³⁻⁶ The dynamics of such movements cause frequency modulations on the back-scattered signal, hence produce shifts in addition to the already present Doppler shift. The extent and characteristics of the Doppler spectra are a function of the targets geometry, dimension, and movement. In essence, the motion-induced Doppler modulation enables the determination of the dynamic properties of objects.

Human gait has complex articulation and reflects radar signals with Doppler modulations that reveal information about motion dynamics. The overall Doppler signature of a moving human, including breathing and heartbeat, which constitutes the biometric radars, has received significant interest during the last few years. Specific applications of biometric radars include the medical investigations, search and rescue, as well as military or law enforcement operations. We note that, in addition to human motions and its importance in localization and tracking of persons, the radar signatures of a stationary human body is also of interest for detection of snipers, injured, or people trapped inside building under fire or under building wreckages. These types of signatures and

bijan.mobasseri@villanova.edu, Telephone: (610) 519-4958

moeness.amin@villanova.edu, Telephone: (610) 519-4599

radar cross-sections were also thoroughly examined and have been developed in many references, including.^{7,8} Measurements of the human body radar response in various frequency bands have appeared in the literature.^{9,10}

Literature in human gait recognition using radar has been often concerned with the processing and extraction of micro Doppler rather than gait recognition or classification. The most effective tool for gait analysis has been joint time-frequency analysis.¹¹ The S-method is proposed to produce sharper micro Doppler features from Wigner distributions.¹² The reassigned joint time-frequency transform is used to sharpen micro Doppler features that normally appear at low resolution in the Short Time Fourier Transform of radar returns.^{13,14} Chirplet transform is used to model radar returns from a walking gait.¹⁵ An acoustic micro Doppler device for the acquisition of gait has also been reported.¹⁶ Scatter plots of stride and appendage/torso ratio vs. velocity are used as gait signature¹⁷ and a linear classifier is built to identify gender and human presence.

This paper considers the classification of the walking motion of humans. It is recognized that the maximum speed of a person walking inside a room is typically 1.5 m/sec which is equivalent to 25 Hz frequency shift when using a Doppler radar at 2.5 GHz. We maintain that the ability to detect human gait depend on the Doppler signature and the power remaining after MTI filtering for clutter removal is applied. The movements of arms and legs give rise to micro Doppler which can be clearly detailed in the time-frequency domain using traditional or modern time-frequency signal representation techniques. We present a minimum distance gait classifier that is trained on feature vectors derived from time-frequency distribution of various gait classes. The classifier can be based on any given time-frequency signal representation method. However, extensive simulations have shown that differences in performance using various quadratic time-frequency distributions for the feature proposed extraction method are insignificant. To this end, we use, in this paper, the simple spectrogram as the domain for feature extractions. Feature vectors are first put through eigendecomposition using principal components analysis (PCA). Each gait is thus defined by its own subspace. For classifying an unknown gait, feature vectors are extracted from the radar return time-frequency representation and then projected onto individual gait subspaces defined during the training phase. The closest gait subspace, in the Mahalanobis distance sense, to the projected vector determines the most likely gait class from which the feature is extracted.

We use real Doppler data measurements and consider one-arm, two-arms and no-arms swinging motions of different human subjects. Data is collected at several different viewing angles. We realize that human gait has been examined,^{7,18,19} and extensive studies in biomechanics have provided an approach to develop a human walking model describing human walking motion with time-dependant body trajectories.^{20,21} However, we chose to employ lab measurement, utilizing the availability of Doppler radar measurements at the Radar Imaging Lab of the Center for Advanced Communications at Villanova University.

2. HUMAN GAIT REPRESENTATION

Gait cycle is defined as human movement between two consecutive heel strikes of the same foot. The cycle is composed of two phases; stance and swing, Fig. 1. Stance phase is the period between heel strike and toe off of the same foot and consists of three phases; heel strike, mid stance and toe off. Swing phase begins when the foot is no longer in contact with the ground and is followed by initial acceleration of the limb followed by deceleration to position the foot for heel strike. Doppler spectrum is a complex response of gait cycle phases to incident radar illumination.

Assume a point target at distance R is moving toward a CW radar at a radial velocity $v(t)$. Even if target's velocity is fixed, its radial component could be changing. If $s(t) = A\cos(2\pi ft)$ is the transmitted signal, the reflected signal is given by $x(t) = A'\cos(2\pi f(t - t_R(t)))$ where $t_R = 2R(t)/c$ is the roundtrip delay time. Range to target is changing according to $R(t) = R_0 - v(t)t$. Therefore, the reflected signal can be written as,

$$x(t) = A'\cos(2\pi f(1 + \frac{2v(t)}{c})t - \frac{4\pi R_0}{c}) \quad (1)$$

The corresponding Doppler shift is $f_d = f.(2v(t)/c)$. Radar returns from the total human body is a superposition of returns from moving arms, legs and feet, each moving with different velocities and acceleration.¹⁶ This return is modeled by,

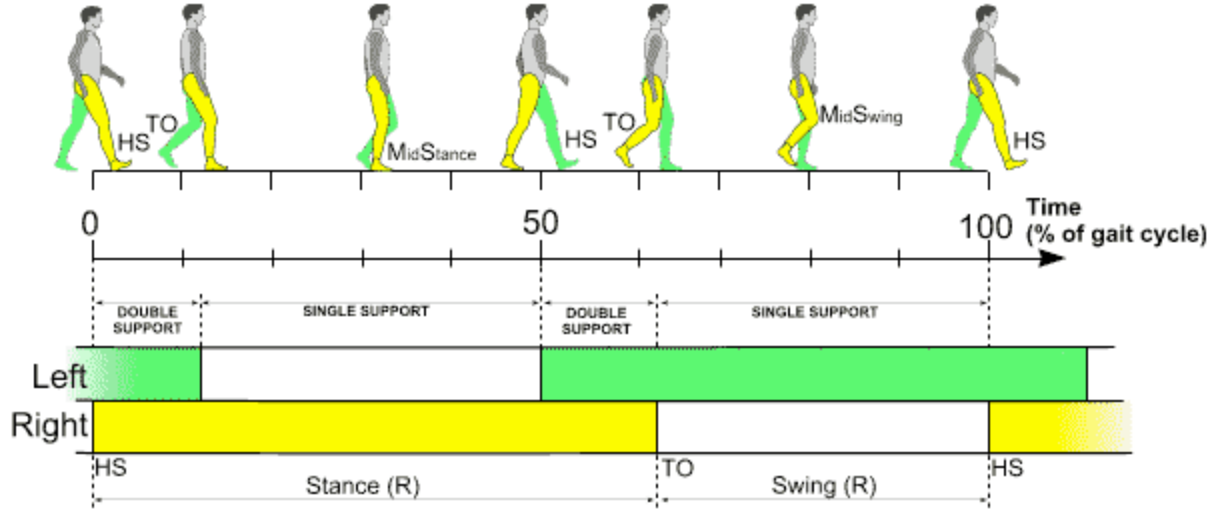


Figure 1. Human gait cycle²²

$$x(t) = \sum_{i=0}^n A'_i \cos(2\pi f(1 + \frac{2v_i(t)}{c})t - \frac{4\pi R_0^i}{c}) \quad (2)$$

where $v_i(t)$ is the radial velocity of the i th limb and R_0^i is the corresponding initial range. Therefore, Doppler shift is a complex interaction of multiple Dopplers originating from individual limbs for which a simple solution is not easily found. Moreover, it is desired to isolate individual Doppler terms arising from arms and legs movements and use them as discriminants. The most effective tool for this purpose is time-frequency analysis techniques such as the Short-Time Fourier Transform (STFT). The STFT of $x(t)$ is given by,

$$STFT(x(t)) = X(t, f) = \int_{-\infty}^{\infty} x(t)w(t - \tau)e^{-j\omega\tau} d\tau \quad (3)$$

where $w(t)$ is a weighting function. We use $|STFT|^2$, the spectrogram, as the source of raw data from which appropriate feature vectors are extracted.

3. SUBSPACE LEARNING FRAMEWORK

The essence of gait classification is to capture the gait cycles unique to individuals or underlying movements. Since stance and swing phases consist of periodic activities, Fourier-based approaches have been widely used. Building upon the success of face recognition, subspace methods have been also been used in image-based gait recognition.²³ However few results are reported for radar-based gait classification. In this section we formulate a subspace learning framework for gait classification using Doppler information.

3.1 Gait Subspace Formation

Let $\mathcal{G} = \{g_1, g_2, \dots, g_M\}$ represent M gait classes. Let $X_k(t, f)$ be the $|STFT|^2$ of g_k . Sample $X_k(t, f)$ on a discrete time-frequency grid $\{t_i, f_j, i = 1, \dots, n, j = 1, \dots, l\}$ to create an $l \times 1$ random vector $\mathbf{X}|g_k$,

$$\mathbf{X}|g_k = [\mathbf{x}_1|g_k, \mathbf{x}_2|g_k, \dots, \mathbf{x}_l|g_k]^T \quad (4)$$

Multiple realizations of $\mathbf{X}|g_k$ are collected in an $l \times n$ data matrix $Z|g_k$, where each column is a measurement of l Doppler frequencies at one time point. Conversely, each column of $Z^T|g_k$ is a measurement of a single Doppler frequency at n time points. The choice of feature vectors is a critical one. The periodicity of the gait is best

captured in $X(t, f_i), \forall t$ whereas large deviations of Doppler due to rapid movement of body parts is best captured by $X(t_i, f), \forall f$. Once (4) is populated, principal component analysis(PCA)²⁴ is used to form individual subspaces for each gait class. PCA is a powerful, nonparametric tool used to discard irrelevant dimensions and keep only the salient features of the data. PCA has been extensively used in image-based gait recognition literature but no results have been reported in the literature for radar-based gait classification.

3.2 Gait Classification

The principal components of $\mathbf{X}|g_k$ are the m dominant eigenvectors of the covariance matrix $C_k = E\{\mathbf{X}|g_k \mathbf{X}^T|g_k\}$. Practically, the estimate of the covariance matrix is computed as $Z|g_k Z^T|g_k$. The matrix of dominant eigenvectors, designated by $\mathbf{P}_k = \{\mathbf{p}_1|g_k, \mathbf{p}_2|g_k, \dots, \mathbf{p}_m|g_k\}^T$, is an $m \times l$ matrix where $m \leq l$ and the i th row $\mathbf{p}_i|g_k$ is the i th eigenvector of C_k . Define Ω_k as the space spanned by \mathbf{P}_k . The projection of data from the i th gait class on the k th subspace is given by,

$$\mathbf{Y}|\omega_i^k = \mathbf{P}_k(\mathbf{X}|g_i - \bar{\mathbf{X}}|g_k), i, k \in \mathbb{N} \quad (5)$$

ω_i^k is the projection of the i th gait class on Ω_k , $\bar{\mathbf{X}}|g_k$ is the mean of the k th gait class, \mathbf{P}_k its eigenvectors and \mathbb{N} is the set of natural numbers less than or equal to M . For $i = k$,

$$E\{\mathbf{Y}|\omega_i^i\} = 0 \quad (6)$$

$$Cov(\mathbf{Y}|\omega_i^i) = \Lambda_i \quad (7)$$

At the conclusion of the PCA step there will be M gait subspaces where on each subspace the other $M - 1$ gait data are projected.

3.3 Gait Classification

Let X be a single feature vector extracted from the spectrogram of an unknown gait. This vector is projected on $\{\Omega_k, k \in \mathbb{N}\}$ per (5) to produce X_k . In each subspace Ω_k compute M distances using the Mahalanobis distance metric,²⁵

$$d_{\Omega_k}^i = d(X_k, \omega_i^k), i, k \in \mathbb{N} \quad (8)$$

Mahalanobis distance is closely related to the maximum likelihood decision rule as the following decision rule applies,

$$if d(X_k, \omega_k^k) < d(X_k, \omega_j^k) \forall j \neq k \in \mathbb{N} \Leftrightarrow X \in g_k \quad (9)$$

To complete classification, repeat (8) in all M subspaces then select the subspace corresponding to the minimum distance. In that subspace select the class to which X_k is closest to. If $X \in g_k$ then the most likely outcome is that the minimum distance occurs in Ω_k . This step generates a label for a single measurement vector. To arrive at a label for the entire gait data, M counters are set up. Every time a feature vector is assigned to a gait class, the corresponding counter is incremented. At the end of the process, the counter with the largest count is the gait class the data is collected from.

4. EXPERIMENTAL RESULTS

Three gait classes were used for experimentation, 1) one-arm swing, 2) two-arms swing and 3) no-arms swing. Data was collected at two incident angles to the walker as shown in Fig. 2. Doppler information for each class was captured by computing the spectrogram of the radar backscatter. Spectrograms of radar backscatter are shown in Fig. 3. The horizontal axis is time and vertical Doppler frequency. Positive and negative Doppler correspond to the subject moving toward or away from the radar, respectively. The spine of each plot corresponds to the torso motion. Even for steady motion the torso speeds up and down during a gait cycle as body goes through gait phases. This phenomenon is reflected in the slowly varying, but strong, Doppler. Arms, legs and foot motions are captured in periodic peaks in the plots. For example, in Fig. 3(b), the large peaks correspond to fast arm motion and the smaller peaks correspond to foot and leg motion. Composite Doppler for the legs, the arms and the feet are captured in Fig. 3(d). Note that the arm motion result in positive and negative Doppler during a gait cycle whereas the leg motion registers positive Doppler only for the approaching subject and negative Doppler for receding subject. The reason is that for the approaching subjects the legs are always moving forward, or are at most stationary, during the double limb support phase. Fig. 3(a), 3(c) and 3(e) show data collected at 30° .

The spectrogram is sampled over a grid of 1024 frequencies by 10,000 time samples. Feature vectors can be defined either as time or frequency slices of the spectrogram. A time slice is a snapshot of the spectrogram capturing 1024 Dopplers frequencies at a given time point. A frequency slice is a snapshot of the spectrogram at one Doppler frequency for 10,000 time points. Either one, or both, can be used in classifier training. Using time snapshots the spectrogram is subsampled to 16×5000 feature vectors. A quarter of the data is used for training and the rest for classification. Training consists of generating subspaces for the three test gait classes using the 5 largest eigenvalues. The 5th largest eigenvalue is only 5% of the peak.

Classifier testing is carried out by classifying feature vectors pulled from known gaits. The first test case captures a male subject walking head-on toward the radar with no arms swinging. Results are shown in Table 1. The first column lists the three gait subspaces. The first row contains the labels assigned by the classifier to the feature vectors. The interpretation of Table 1 is as follows. When feature vectors from the no-arms swing gait are projected on the one-arm subspace, 30% are labeled as one-arm swing, 4.2% as two-arms swing and 66% as no-arms swing. The same feature vectors are projected on the remaining gait subspaces and classified to one of three classes. The unknown gait belongs to the subspace with the highest correct classification rate. In this case the no-arms swing data is classified to the no-arms gait 82.5% of the time when projected on the no-arms swing gait space. This is a higher rate than any other projection. The second and third rows represent the classification rates as found in the remaining subspaces. In general, the highest classification rate is achieved when data is projected on its own subspace. Therefore, only one diagonal element is expected to show a peak and the corresponding column label is the unknown gait. If the peak is off diagonal then either the unknown gait is not in the training set or it is misclassified due to view angle or other departures from the training set. Tables 2 and 3 show similar results for the one-arm and two-arms swing gaits. In all three cases the unknown gait is correctly classified.

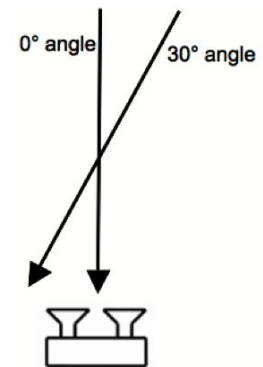
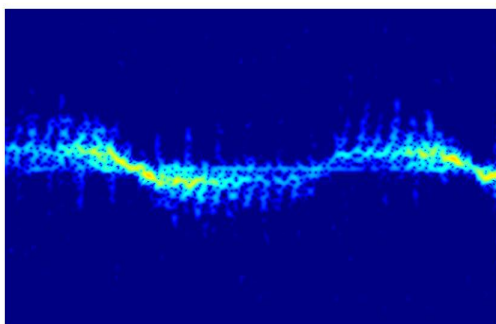


Figure 2. Data is collected with two angles of incidence relative to the walker.

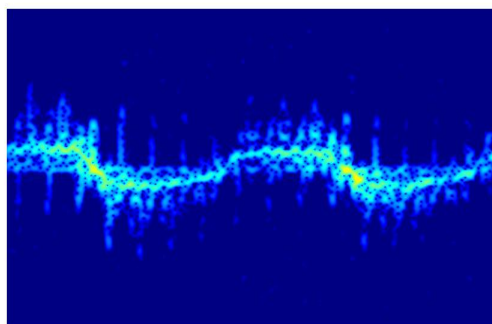
Table 1. Unknown gait. No-arms swing at 0°

	labeled One arm	labeled Two arms	labeled No arms
One arm	30%	4.2%	66%
Two arms	8.7%	18.7%	72.6%
No arms	13.7%	3.9%	82.5%

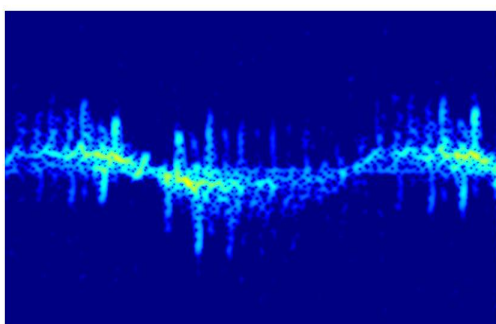
We have also trained and tested the classifier using feature vectors that are snapshots of Doppler for all time. Such feature vectors capture periodic structure of the gait cycle. Tables 4-6 show the classification results. When



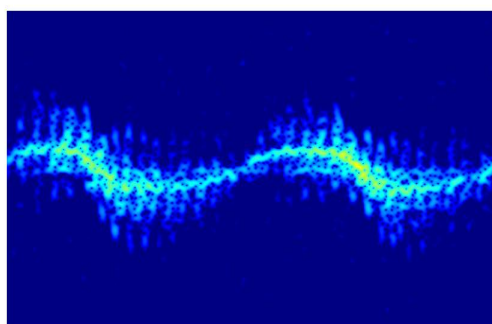
(a) One-arm swing gait at 30°



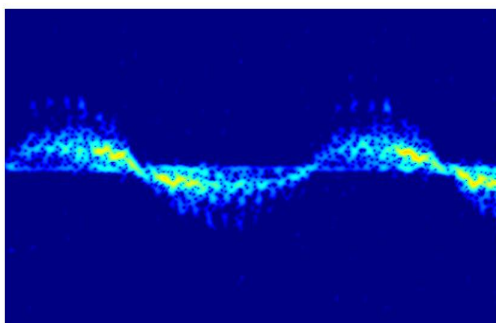
(b) One-arm swing gait at 0°



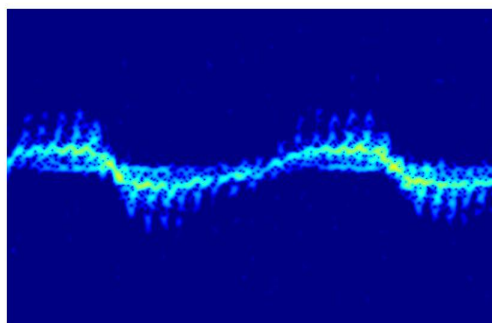
(c) Two-arms swing gait at 30°



(d) Two-arms swing gait at 0°



(e) No-arms swing gait at 30°



(f) No-arms swing gait at 0°

Figure 3. Spectrogram of three different gaits captured at two incidence angles. It is clear that occlusion of the body makes identification of gaits prone to error. For example, the two arms swing at 30° is more similar to the one arm swing at 0° than the two arm swing at 0°

an unknown gait is projected on its own subspace, feature vectors are classified to the correct gait class at much higher rates compared to time snapshot feature vectors. However, other on-diagonal elements are quite high as well. Although correct classification is still achieved, the error margins are smaller.

Table 2. Unknown gait. One-arm swing at 0°

	labeled One arm	labeled Two arms	labeled No arms
One arm	69.1%	11.9%	19%
Two arms	44.3%	32.7%	22.9%
No arms	45.9%	17.8%	36.3%

Table 3. Unknown gait. Two-arms swing at 0°

	labeled One arm	labeled Two arms	labeled No arms
One arm	39.4%	44.8%	15.8%
Two arms	9.2%	70.7%	20.2%
No arms	19.3%	44.8%	35.9%

Table 4. Unknown gait. One-arm swing(Doppler snapshots)

	labeled one arm	labeled two arms	labeled no arms
One arm	100%	0%	0%
Two arms	5.94%	94.1%	0%
No arms	4.51%	1.19%	94.3%

Table 5. Unknown gait. Two-arms swing(Doppler snapshots)

	labeled one arm	labeled two arms	labeled no arms
One arm	89.3%	10.7%	0%
Two arms	0%	98.3%	1.66%
No arms	0%	2.38%	97.6%

Table 6. Unknown gait. No-arms swing(Doppler snapshots)

	labeled One arm	labeled two arms	labeled no arms
One arm	78.6%	0%	21.4%
Two arms	0%	90.5%	9.5%
No arms	0%	0%	100%

The classifier is so far trained on data collected for head-on views. However, actual view angles are unpredictable. To evaluate classifier performance data is collected for motion at 30° angle to the axis of antenna. As the direction of motion moves away from the antenna axis, the arms get progressively occluded by the body and the gait begins to acquire the signature of a no-arms swing. In Table 7 the highest diagonal corresponds to the no-arms swing gait, which is in error. A one-arm gait has been classified as a no-arms gait. Interestingly, the two-arms swing gait viewed at 30° is still correctly classified, Table 8. Apparently, the body has not completely occlude both arms.

Table 7. Unknown gait. One-arm swing at 30°

	labeled one arm	labeled two arms	labeled no arms
One arm	42.9%	11.9%	45.1%
Two arms	15.1%	36.6%	48.3%
No arms	18.7%	14.8%	66.5%

Table 8. Unknown gait. Two-arms swing at 30°

	labeled 1arm	labeled 2arm	labeled noarms
1arm	49.3%	28%	22.7%
2arm	13.1%	59.1%	27.8%
noarms	18.8%	36.6%	44.6%

5. CONCLUSIONS

Doppler frequency of radar backscatter contains signatures that can be used to classify gait. We demonstrated a subspace learning method using PCA eignedeecomposition. The approach extracts feature vectors from the magnitude of short time frequency transform of radar returns and used in a minimum distance classifier. The PCA classifier was specifically tested to determine the state of the swinging of the arms of a walking human. This becomes important for assessing possible scenarios of confined or restricted human arms, such as presence of hostages or people carrying of relatively heavy items with single or both hands. Initial results indicate that this approach is simple, fast and effective. Further work calls for the comparison with the neural network based classifiers and the use of data collected through the wall for investigating wall robustness issues.

REFERENCES

- [1] V. Chen, F. Li, S.-S. Ho, and H. Wechsler, "Analysis of micro-doppler signatures," *Radar, Sonar and Navigation, IEE Proceedings -* **150**, pp. 271–6–, Aug. 2003.
- [2] V. Chen, "Detection and analysis of human motion by radar," *Radar Conference, 2008. RADAR '08. IEEE*, pp. 1–4, May 2008.
- [3] R. Kleinman and R. Mack, "Scattering by linearly vibrating objects," *Antennas and Propagation, IEEE Transactions on* **27**, pp. 344–352, May 1979.
- [4] J. Gray, "The doppler spectrum for accelerating objects," *Radar Conference, 1990., Record of the IEEE 1990 International*, pp. 385–390, May 1990.
- [5] P. Setlur, F. Ahmad, and M. Amin, "Analysis of micro-doppler signals using linear fm basis decomposition," *Radar Sensor Technology X* **6210**(1), p. 62100M, SPIE, 2006.
- [6] P. Setlur, M. Amin, and F. Ahmad, "Urban target classifications using time-frequency micro-doppler signatures," *Signal Processing and Its Applications, 2007. ISSPA 2007. 9th International Symposium on*, pp. 1–4, Feb. 2007.
- [7] T. Dogaru, L. Nguyen, and C. Le, "Computer models of the human body signature for sensing through the wall radar applications," Technical Report ARL-TR-4290, ARL, Adelphi, MD, Sep. 2007.

- [8] C. Le and T. Dogaru, "Numerical modeling of the airborne radar signature of dismount personnel in the uhf-, l-, ku- and ka-bands," Technical Report ARL-TR-4336, ARL, Adelphi, MD, Dec. 2007.
- [9] A. Tan and M. Chia, "Measuring human body impulse response using uwb radar," *Electronics Letters* **41**, pp. 1193–1194, Oct. 2005.
- [10] N. Yamada, "Radar cross section for pedestrian in 76 ghz band," Research Report 4, Toyota CRDL, 2004.
- [11] V. C. Chen, "Joint time-frequency analysis for radar signal and imaging," *IEEE International Geoscience and Remote Sensing Symposium, 2007. IGARSS 2007*, pp. 5166–5169, July 2007.
- [12] T. Thayaparan and L. Stankovic and I. Djurovic, "Micro-doppler-based target detection and feature extraction in indoor and outdoor environments," *Journal of the Franklin Institute* **345**(6), pp. 700–722, 2008.
- [13] S.S. Ram and H. Ling, "Analysis of microDopplers from human gait using reassigned joint time-frequency transform," *Electronic Letters* **43**, May 2007.
- [14] S. S. Ram, Y. Li, A. Lin, H. Ling, "Doppler-based detection and tracking of humans in indoor environments," *Journal of The Franklin Institute* **345**(6), pp. 679–699, 2008.
- [15] J. L. Geisheimer, W. S. Marshall and E. Greneker, "A continuous-wave (CW) radar for gait analysis," *Thirty-Fifth Asilomar Conference on Signals, Systems and Computers*, pp. 834–838, 2001.
- [16] Z. Zhang, P. Pouliquen, A. Waxman and A. Andreou, "Acoustic micro-doppler radar for human gait imaging," *J Acoust Soc Am* **121**, pp. 110–113, March 2007.
- [17] M. Otero, "Application of a continuous wave radar for human gait recognition," in *Society of Photo-Optical Instrumentation Engineers (SPIE) Conference Series*, **5809**, pp. 538–548, 2005.
- [18] P. van Dorp and F. Groen, "Human walking estimation with radar," *Radar, Sonar and Navigation, IEE Proceedings -* **150**, pp. 356–365, Oct. 2003.
- [19] J. Geisheimer, E. Greneker, and W. Marshall, "High-resolution doppler model of the human gait," *Radar Sensor Technology and Data Visualization*, SPIE, Apr. 2002.
- [20] P. Van Dorp and F. C. Groen, "Human walking estimation with radar," *IEE Proc. Radar Sonar Navig* **150**, pp. 356–365, 2003.
- [21] R. Boulic, M. N. Thalmann and D. Thalmann, "A global human walking model with real-time kinematic personification," *Visual Computer* (6), pp. 344–358, 1990.
- [22] "Biomechanis." <http://www.sportspodiatry.co.uk/biomechanics.htm>, March 2009.
- [23] Chiraz BenAbdelkader and Ross Cutler and Harsh Nanda and Larry S. Davis, "EigenGait: Motion-Based Recognition of People Using Image Self-Similarity," in *AVBPA '01: Proceedings of the Third International Conference on Audio- and Video-Based Biometric Person Authentication*, pp. 284–294, Springer-Verlag, 2001.
- [24] J. Shlens, "A tutorial on principal component analysis." <http://www.sn1.salk.edu/shlens/pub/notes/pca.pdf>, December 2005.
- [25] R. O. Duda and P. E. Hart, *Pattern Classification*, Wiley, 2nd ed., 2000.